

# A Simple Model Parameter Extraction Methodology for an On-Chip Spiral Inductor

Nam-Jin Oh and Sang-Gug Lee

**ABSTRACT**—In this letter, a simple model parameter extraction methodology for an on-chip spiral inductor is proposed based on a wide-band inductor model that incorporates parallel inductance and resistance to model skin and proximity effects, and capacitance to model the decrease in series resistance above the frequency near the peak quality factor. The wide-band inductor model does not require any frequency dependent elements, and model parameters can be extracted directly from the measured data with some curve fitting. The validity of the proposed model and parameter extraction methodology are verified with various size inductors fabricated using 0.18  $\mu\text{m}$  CMOS technology.

**Keywords**—Inductor; inductor model, skin effect, series resistance, series inductance, substrate resistance, substrate modeling.

## I. Introduction

An on-chip spiral inductor is an important component for radio frequency integrated circuits (RFICs) such as low-noise amplifiers, voltage-controlled oscillators, and impedance-matching networks. Many works have been done on on-chip inductor design and modeling. Accuracy in the inductor model is an important part of RFIC design. An inaccurate model for the on-chip inductor leads to incorrect RFIC performances, long turn-around time, and time-to-market delay.

In particular, as operation frequency goes up and frequency bandwidth widens, an accurate inductor model is indispensable for RFIC designers. Figure 1 shows a conventional nine-element  $\pi$ -model. However, the model has difficulty in modeling skin and proximity effects, as well as drop-down

characteristics of effective series resistance  $R_{series}$  at high frequencies. Figure 2 compares measured and conventionally modeled characteristics of the quality factor and effective series

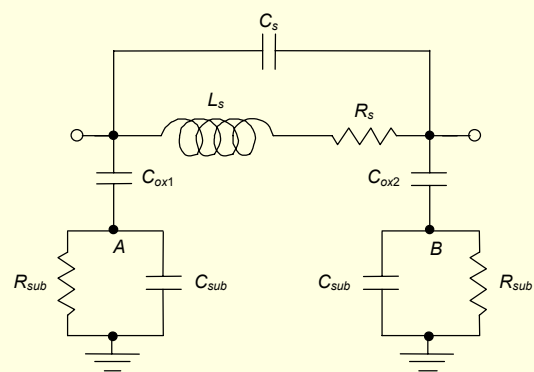


Fig. 1. Conventional nine-element  $\pi$ -type inductor model.

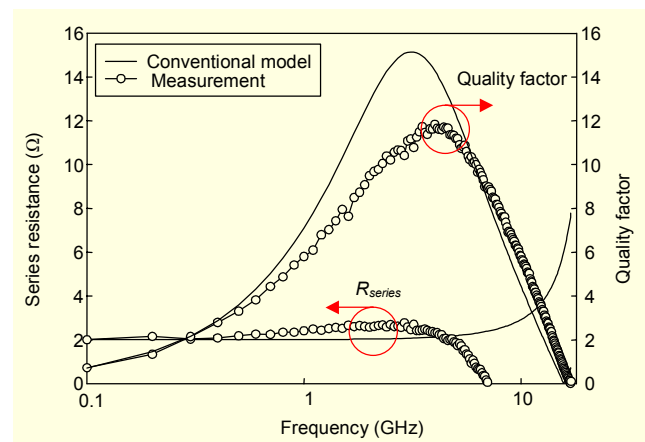


Fig. 2. Measured and conventionally modeled effective series resistance and quality factor of a 2.5-turn square spiral inductor as a function of frequency.

Manuscript received July 18, 2005; revised Oct. 14, 2005.

This work was supported in part by the Korean Intellectual Property Office (KIPO).

Nam-Jin Oh (phone: +82 42 866 6284, email: onamjin@icu.ac.kr) and Sang-Gug Lee (email: sglee@icu.ac.kr) are with the School of Engineering, Information and Communications University, Daejeon, Korea.

resistance of an inductor. In the measurement data, the effective series resistance increases as the frequency goes up mainly due to the skin and proximity effects, and drops down abruptly above the frequency of the peak quality (Q) factor up to the self resonance frequency (SRF) of the inductor. However, assuming that the inductor model uses only frequency independent elements, the conventional nine-element  $\pi$ -model leads to flat effective resistance  $R_{series}$  up to the frequency of the peak Q factor, thereby resulting in an overly optimistic higher Q factor at the frequency of peak Q compared to that of the measurement. In the conventional model, modifying  $R_s$  in Fig. 1 as a frequency dependent resistor enables the accommodation of skin and proximity effects, which results in an increase in the series resistance near peak Q [1], [2]. However, frequency dependent elements are complicated to implement in typical circuit simulators, especially time domain SPICE-like simulators [3].

As an alternative, others have tried adding a series  $L_{sk}-R_{sk}$  in parallel with  $R_s$  to model the skin and proximity effects, in addition to a parallel  $R-C$  between nodes A and B in Fig. 1 to model the lateral substrate coupling, while capacitor  $C_s$  is eliminated [4]. But this alternative approach requires some elaboration (to extract the series resistance at low frequencies near DC, a parallel combination of  $R_{sk}$  and  $R_s$  should be calculated) and optimization to extract the model parameters for skin and proximity effects from the measurement, and excludes the port-to-port series capacitance  $C_s$ . Another approach includes an additional parallel  $L_{sk}-R_{sk}$  in series with  $L_s$  and  $R_s$  to model the skin and proximity effects [5], but this approach does not predict the drop-down characteristics of  $R_{series}$  at higher frequencies. Even though the approach in [2], which has been constructed using a two-element  $\pi$ -model, can predict the drop-down characteristics of series resistance at a higher frequency, it is somewhat complicated to implement in circuit simulators.

In this letter, a new modified inductor model is proposed that aims at implementing a simple direct equivalent model parameter extraction methodology with just some curve fitting (that is, one that does not require a rigorous optimization routine). The model accurately reflects the skin and proximity effects, as well as the drop-down characteristics of effective series resistance in the frequency range from DC to the SRF. Section II introduces a new modified inductor model and explains the direct model parameter extraction methodology step by step. Section III verifies the validity of the model compared to the measurement, and section IV concludes this work.

## II. Direct Model Parameter Extraction Methodology

Figure 3 shows the proposed wide-band inductor model that requires only frequency independent elements. Three more elements are added to the conventional nine-element  $\pi$ -model,

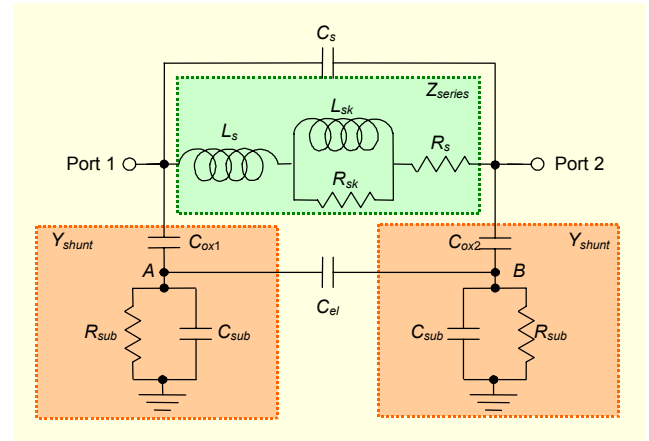


Fig. 3. Proposed twelve-element  $\pi$ -type inductor model.

of which the parallel  $L_{sk}-R_{sk}$  is used to represent the skin and proximity effects, and the lateral substrate coupling capacitance  $C_{el}$  to reflect the drop-down characteristics of the effective resistance  $R_{series}$ .

From Fig. 3, with the exception of  $C_s$  and  $C_{el}$ , all other parameters can be extracted directly from the measurement results. The extraction of  $L_s$ ,  $L_{sk}$ ,  $R_s$ , and  $R_{sk}$  can be done as follows. From the two-port spiral inductor model shown in Fig. 3,  $Z_{series}$  can be given by

$$Z_{series}(\omega) = R_s + \frac{\omega^2 L_{sk}^2 R_{sk}}{\omega^2 L_{sk}^2 + R_{sk}^2} + j\omega \left( L_s + \frac{L_{sk} R_{sk}^2}{\omega^2 L_{sk}^2 + R_{sk}^2} \right). \quad (1)$$

At frequencies where the effects of  $C_s$  and  $C_{el}$  are negligible, the series impedance  $Z_{series}$  is approximately equal to  $-1/Y_{21}$ .

$$Z_{series}(\omega) \approx -\frac{1}{Y_{21}} = R_{series}(\omega) + j\omega L_{series}(\omega), \quad (2)$$

where  $R_{series}$  is the frequency dependent effective series resistance and  $L_{series}$  the effective series inductance. From (1) and (2), the effective series resistance  $R_{series}$  is equal to  $R_s$  near DC, and approaches  $R_s + R_{sk}$  at the SRF; likewise, the effective inductance  $L_{series}$  is equal to  $L_s + L_{sk}$  near DC, and converges to  $L_s$  at the SRF. Figure 4 shows the measured and modeled  $R_{series}$  and  $L_{series}$  for a 2.5 turn spiral inductor. In Fig. 4, the measured  $R_{series}$  increases mainly due to the skin and proximity effects [2] as the frequency increases, and then drops quickly at higher frequency due to the lateral substrate coupling capacitance  $C_{el}$ .

The measured  $L_{series}$  decreases up to the point where  $R_{series}$  peaks, and then increases quickly at higher frequencies due to the series coupling capacitance,  $C_s$ . As shown in Fig. 4, while the capacitances  $C_s$  and  $C_{el}$  are being deactivated in the model, knowing the values for  $R_s$  and  $L_s + L_{sk}$ , and utilizing the measurement data below the  $R_{series}$  peak, the model can be

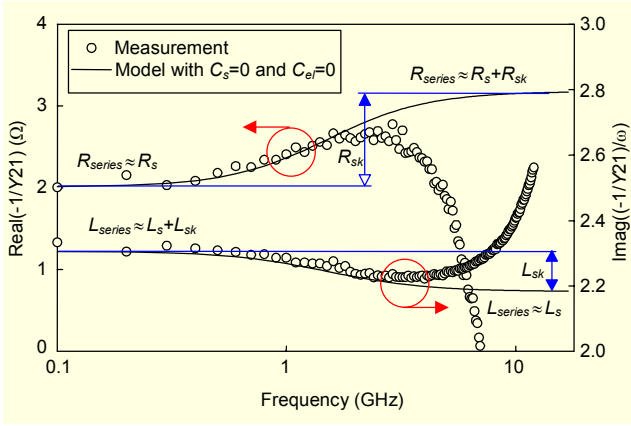


Fig. 4. Measured effective series resistance and inductance as a function of frequency along with model parameter extraction scheme.

fitted to the measurement by a simple adjustment of  $R_{sk}$  and  $L_{sk}$ . Therefore, based on the measurement data and a simple adjustment, the series parameters  $L_s$ ,  $L_{sk}$ ,  $R_s$ , and  $R_{sk}$  are extracted.

From the inductor model shown in Fig. 3,  $Y_{shunt}$  can be given by

$$\frac{1}{Y_{shunt}(\omega)} = \frac{R_{sub}}{1 + \omega^2 R_{sub}^2 C_{sub}^2} + \frac{1}{j\omega C_{ox} \left( \frac{1 + \omega^2 R_{sub}^2 C_{sub}^2}{1 + \omega^2 R_{sub}^2 C_{sub}^2 (C_{sub} + C_{ox})} \right)}$$

$$= R_{shunt}(\omega) + \frac{1}{j\omega C_{shunt}(\omega)}. \quad (3)$$

From Fig. 3, while the capacitances  $C_s$  and  $C_{el}$  are being deactivated in the model, the shunt admittance  $Y_{shunt}$  is approximately equal to  $Y_{11} + Y_{21}$ , and

$$Y_{shunt}(\omega) \approx Y_{11} + Y_{21}. \quad (4)$$

Therefore, using the measured values of  $Y_{11}$  and  $Y_{21}$ , and based on (3) and (4),  $R_{shunt}$  and  $C_{shunt}$  can be plotted as a function of frequency as shown in Fig. 5. From (3),  $R_{shunt}$  and  $C_{shunt}$  are equal to  $R_{sub}$  and  $C_{ox}$ , respectively, near DC; and  $C_{shunt}$  approaches the value of  $C_{ox}C_{sub}/(C_{ox} + C_{sub})$  at the SRF.

The last two parameters of the model in Fig. 3, the lateral substrate coupling capacitance  $C_{el}$  and the port-to-port series capacitance  $C_s$ , are decided by fitting the model to the measurement. By increasing  $C_{el}$ , the effective series resistance and the effective series inductance approach the measured data. The last parameter  $C_s$  is decided by fitting the modeled quality factor to that of the measurement.

The quality factor of an inductor is given by

$$Q = -\frac{\text{imag}(Y_{11})}{\text{real}(Y_{11})}. \quad (5)$$

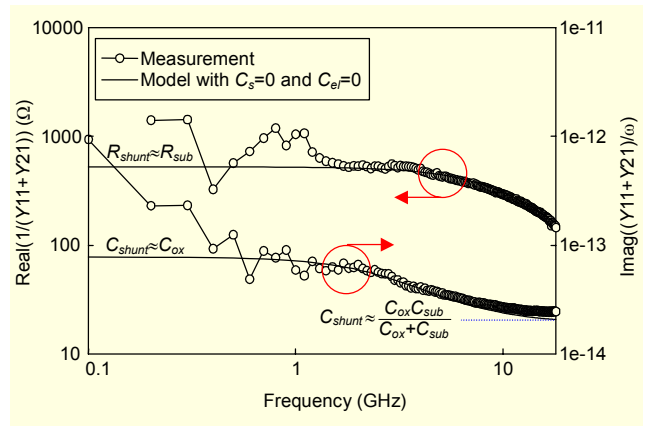


Fig. 5.  $R_{shunt}$  and  $C_{shunt}$  plotted as a function of frequency from the measured  $Y_{11} + Y_{21}$  along with the model parameter extraction scheme.

The values of  $C_{el}$  and  $C_s$  determine the frequency behavior of  $R_{series}$  and  $L_{series}$ , respectively, above the frequency of peak  $Q$ .

### III. Verification of Model and Extraction Scheme

To verify the validity of the model and extraction scheme, square spiral inductors with various geometries are fabricated using 0.18  $\mu\text{m}$  CMOS technology. A 2  $\mu\text{m}$  thick top metal is used for the better quality factor, and the resistivity of the silicon substrate is about 10  $\Omega \cdot \text{cm}$ . The fabricated inductor metal width, spacing, and inner diameter are 15, 1.5, and 120  $\mu\text{m}$ , respectively. The two-port S-parameters of the inductors are measured using a network analyzer and RF probes. For de-embedding, just an open pad structure is used since the short pad structure does not change the calibration results very much in the frequency range from DC to the SRF [6]. The model parameters are extracted following the steps described in section II without running a rigorous optimization routine. Figure 6 shows the measured and modeled inductances, quality factors, and resistances for 2.5, 3.5, 4.5, and 5.5 turn inductors over a wide frequency band of interest. As can be seen in Fig. 6, the model shows very good agreement with the measured data over a wide range of frequencies.

### IV. Conclusion

A new wide-band inductor model is proposed that incorporates both an additional parallel  $L$ - $R$  element to model skin and proximity effects, and a lateral substrate coupling capacitance to model the decrease in effective series resistance at higher frequencies. As the model requires no frequency dependent elements, it can easily be implemented in circuit simulators. The parameters of the proposed model can be

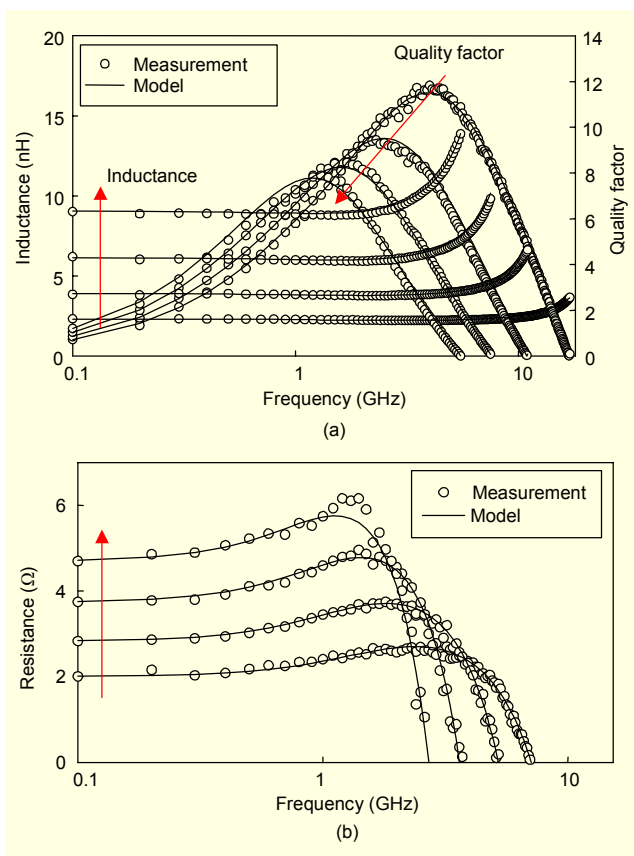


Fig. 6. Measured and modeled (a) inductance and quality factor, and (b) resistance for 2.5, 3.5, 4.5, and 5.5 turn inductors. The arrows indicate an increase in the number of turns.

extracted directly from the measured  $Y$ -parameters using the proposed simple extraction scheme with some curve fitting. The validity of the proposed model and extraction scheme has been successfully verified with various sizes of inductors fabricated using  $0.18\ \mu\text{m}$  CMOS technology.

## References

- [1] C. P. Yue and S. S. Wong, "Physical Modeling of Spiral Inductors on Silicon," *IEEE Trans. Electron Devices*, vol. 47, Mar. 2000, pp. 560-568.
- [2] Y. Cao, R. A. Groves, N. D. Zamdmer, J.-O. Plouchart, R. A. Wachnik, X. Huang, T.-J. King, and C. Hu, "Frequency-Dependent Equivalent Circuit Model for On-Chip Spiral Inductors," *IEEE Custom Integrated Circuits Conf.*, 2002, pp. 217-220.
- [3] T. Kamgaing, T. Myers, M. Petras, and M. Miller, "Modeling of Frequency Dependent Losses in Two-Port and Three-Port Inductors on Silicon," *IEEE MTT-S Int. Microwave Symp. Dig.*, 2002, pp. 153-156.
- [4] J. Gil and H. Shin, "A Simple Wide-Band On-Chip Inductor Model for Silicon-Based RF ICs," *IEEE Trans. Microwave*

*Theory Tech.*, vol. 51, Sep. 2003, pp. 2023-2028.

- [5] C.-J. Chao, S.-C. Wong, C.-J. Kao, M.-J. Chen, L.-Y. Leu, and K.-Y. Chiu, "Characterization and Modeling of On-Chip Spiral Inductors for Si RFICs," *IEEE Trans. Semiconductor Manufacturing*, vol. 15, Feb. 2002, pp. 19-29.
- [6] T. Ytterdal, Y. Cheng, and T. A. Fjeldly, *Device Modeling for Analog and RF CMOS Circuit Design*, John Wiley & Sons Ltd, The Atrium, England, 2003.